Structural analysis of nucleosomal barrier to transcription

Daria A. Gaykalova[a,1,2], Olga I. Kulaeva[b,2], Olesya Volokh[c,2], Alexey K. Shaytan[c], Fu-Kai Hsieh[a], Mikhail P. Kirpichnikov[c], Olga S. Sokolova[c], and Vasily M. Studitsky[a,b,c,3]

[a]Department of Pharmacology, Rutgers University School of Medicine, Piscataway, NJ 08854; [b]Cancer Epigenetics Program, Fox Chase Cancer Center, Philadelphia, PA 19111; and [c]Biology Faculty, Lomonosov Moscow State University, Moscow, Russia 119991

Edited by Gary Felsenfeld, National Institutes of Health, Bethesda, MD, and approved September 14, 2015 (received for review April 28, 2015)

Thousands of human and *Drosophila* genes are regulated at the level of transcript elongation and nucleosomes are likely targets for this regulation. However, the molecular mechanisms of formation of the nucleosomal barrier to transcribing RNA polymerase II (Pol II) and nucleosome survival during/after transcription remain unknown. Here we show that both DNA–histone interactions and Pol II backtracking contribute to formation of the barrier and that nucleosome survival during transcription likely occurs through allosterically stabilized histone–histone interactions. Structural analysis indicates that after Pol II encounters the barrier, the enzyme backtracks and nucleosomal DNA recoils on the octamer, locking Pol II in the arrested state. DNA is displaced from one of the H2A/H2B dimers that remains associated with the octamer. The data reveal the importance of intranucleosomal DNA–protein and protein–protein interactions during conformational changes in the nucleosome structure on transcription. Mechanisms of nucleosomal barrier formation and nucleosome survival during transcription are proposed.

transcription | elongation | chromatin | backtracking | RNA polymerase II

RNA polymerase II (Pol II) transcription induces extensive chromatin remodeling accompanied by histone covalent modifications and exchange (refs. 1–3 for review). At the same time, histones are evicted only from highly transcribed genes (4–6); thus Pol II typically encounters nucleosomes during transcription of every ∼200-bp DNA region. Nucleosomes remaining on transcribed genes form two types of barriers for transcribing Pol II (2, 7). First, each nucleosome presents a barrier where Pol II is paused after transcribing 40–50 bp from the promoter–proximal nucleosome boundary (2). Second, a much higher barrier is formed by the first (+1) transcribed nucleosome in *Drosophila* (7); in this case Pol II is stalled at the nucleosomal boundary. Stalled Pol II was detected on many genes: from 15% to over 50% of genes in flies and humans, respectively (8–10). In many cases the paused Pol II was comapped with first, well-positioned +1 nucleosome, suggesting that this nucleosome could dictate the pausing and overall level of gene expression (7, 11).

In vitro data have established that a single nucleosome can form a high barrier for Pol II transcription of the first type (12–17) and that transcription factors, histone chaperones, histone modifications, and/or multiple molecules of Pol II are required to overcome the barrier (14, 15, 18–26). The strong barrier is formed after transcribing 40–50 bp past the nucleosome boundary [the +(40–50) region], is nucleosome specific, Pol II specific, and was described for all analyzed organisms, from yeast to human (13–15). Thus, the +40–50 nucleosomal barrier is a "universal" signature of transcription through chromatin by Pol II and could be used for gene regulation at the level of transcript elongation (14). On any given DNA sequence, the barrier forms in distinct positions within the +(40–50) region (14).

In this work, to analyze the molecular mechanism of formation of the high barrier to transcription, we have studied the outcome of the encounter between Pol II and nucleosomes in vitro. Biochemical and structural analyses (the structural analysis has been conducted using *Escherichia coli* RNA polymerase as a model) revealed that after encountering the strong nucleosomal barrier, the elongation complex is converted into a backtracked state on nucleosomal templates. Pol II backtracks up to 6 bp and induces recoiling of nucleosomal DNA on the histone octamer. The nucleosome-specific arrest of Pol II is stable, but is fully reversible upon removal of core histones from DNA.

Results

Experimental Strategy. Our experiments were conducted using mononucleosomal templates that recapitulate many important aspects of the Pol II-type mechanism of chromatin transcription in vivo (21, 27, 28). The mechanism of formation of the nucleosomal barrier to transcription was studied using the 601 and 603 mononucleosomes (Fig. S1*A*) that contain a polar barrier DNA sequence (PBS) and form a very strong nucleosomal barrier in one of the two transcriptional orientations (nonpermissive orientation) (14, 16, 29). The templates were designed to allow stalling of Pol II at the positions −41 and −5 (41 or 5 bp upstream of the promoter–proximal nucleosomal boundary) in the presence of various partial combinations of NTPs (Fig. S1*A*). Pol II is spontaneously arrested during transcription of the nonpermissive 601 nucleosome at 150 mM KCl at the +46 and +48 positions (Fig. S1*B*). The arrest is reversible, as Pol II can transcribe the entire template upon histone octamer destabilization at 1 M KCl (Fig. S1*B*).

Significance

On the majority of eukaryotic genes RNA polymerase II meets nucleosomes during transcription of every ∼200 bp of DNA. The key features of Pol II–nucleosome encounter are conserved from yeast to human, but the molecular mechanism of this process remains unknown. Our data suggest a mechanism of formation of the high nucleosomal barrier to Pol II that participates in regulation of transcript elongation in eukaryotes. The proposed mechanism explains the remarkable efficiency of nucleosome survival during transcription, important for maintenance of epigenetic and regulatory histone modifications. Similar mechanisms are likely used during various other DNA transactions, including DNA replication and ATP-dependent chromatin remodeling. Some factors involved in chromatin transcription (e.g., FACT and PARP) participate in cancer development/aging.

Author contributions: O.I.K., M.P.K., O.S.S., and V.M.S. designed research; D.A.G., O.I.K., O.V., A.K.S., F.-K.H., O.S.S., and V.M.S. performed research; D.A.G., O.I.K., O.V., A.K.S., F.-K.H., M.P.K., O.S.S., and V.M.S. analyzed data; and D.A.G. and V.M.S. wrote the paper.

The authors declare no conflict of interest.

This article is a PNAS Direct Submission.

[1]Present address: Department of Otolaryngology, Johns Hopkins University, Baltimore, MD 21231.

[2]D.A.G., O.I.K., and O.V. contributed equally to this work.

[3]To whom correspondence should be addressed. Email: vasily.studitsky@fccc.edu.

This article contains supporting information online at www.pnas.org/lookup/suppl/doi:10.1073/pnas.1508371112/-/DCSupplemental.

The PBS-R3 Sequence Dictates the High Nucleosomal Barrier to Transcription. For initial analysis of the nucleosomal barrier, we have conducted detailed mutagenesis of the PBS +(87–102, regions R1–R3, Fig. 1*A*) region that dictates the height of the nucleosomal barrier to transcription (16). The 603 template was selected for this study because its PBS sequence was recently mapped (16).

The effect of mutations in R1, R2, and R3 subregions of the PBS on the affinity to core histones to DNA and the barrier to Pol II transcription were analyzed (Fig. 1 and Fig. S2). Only mutations in the 603-R2 sequence result in a strong decrease of the high affinity to histones (Fig. 1 *A* and *B* and Fig. S2*A*). Note that none of the individual sets of R mutations (R1, R2, or R3) alone affects the mobility of the nucleosomes in the native gel that indicates identical nucleosome positioning on the template (Fig. S2*A*) (16). Surprisingly, the R2 mutations only minimally affect the height of nucleosomal barrier to transcription, determined primarily by the promoter–distal R3 +(99–102) sequence (Fig. 1*B* and Fig. S2*B*).

Previously we have proposed that the nucleosomal barrier is relieved as a result of uncoiling of ∼100-bp DNA region in front of the enzyme after formation of a small, Pol II-containing DNA loop on the surface of histone octamer (Ø loop) (Fig. 1*C*) (16, 30). Our current data support this model, because otherwise it is very difficult to explain how the R3 sequence can affect the nucleosomal barrier to Pol II formed almost 60 bp upstream of

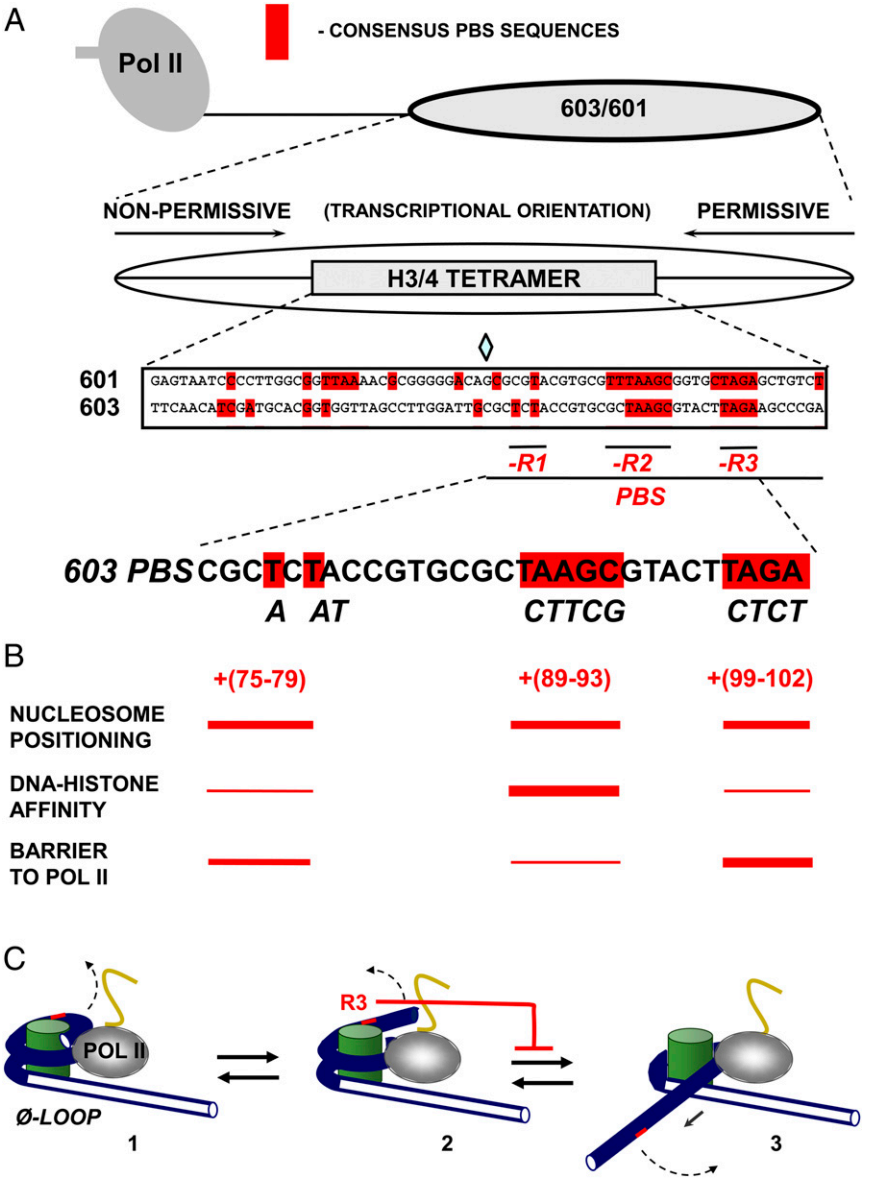

Fig. 1. The R3 sequence dictates the strength of the polar barrier to transcription by Pol II. (*A*) Polar distribution of the polar barrier sequences (PBSs) within the nucleosomal DNA. The 601 and 603 sequences forming polar barriers to Pol II transcription are aligned according to their transcriptional orientations (permissive or nonpermissive). The regions of the 603 DNA where the sequence changes were introduced on different variants of the template (-R1, -R2, or -R3, shown in italics) are underlined. The nucleosomal dyad is indicated. In this work, all nucleosomes were transcribed in nonpermissive orientation. (*B*) Effect of mutations in the 603 -R1, -R2, or -R3 sequences on nucleosome-positioning properties, DNA–histone affinities, and the strength of the nucleosomal barrier to transcription. The thickness of the lines is directly proportional to the magnitude of the effect. See Fig. S2 for quantitative analysis. (*C*) After formation of a small intranucleosomal DNA loop on the surface of the nucleosome (*1*), Pol II likely initiates uncoiling of nucleosomal DNA, starting from the promoter–distal end (*2*), and eventually involving all nucleosomal DNA in front of the enzyme (*3*).

R3. Because R3 is the most promoter–distal sequence, the data also suggest that uncoiling of the promoter–distal 100-bp region of nucleosomal DNA after Ø-loop formation is initiated at the promoter–distal end of nucleosomal DNA (Fig. 1*C*).

Taken together with our previous data (16), our current results suggest that all three R sequences cooperatively contribute to nucleosome positioning, R2 is primarily responsible for DNA–histone affinity, and R3 is largely responsible for the height of the nucleosomal barrier to transcription. Uncoiling of downstream DNA is likely initiated from the promoter–distal end of nucleosomal DNA.

Pol II Backtracks in the Arrested Complexes and Displaces Upstream DNA from the Octamer. The state of Pol II after encountering the high nucleosomal barrier was addressed using the 601 template that presents the strongest nucleosomal barrier to transcribing Pol II (14) (Fig. 2*A*). Pol II was spontaneously arrested at the positions +46 and +48 on the 601-nucleosomal template (Fig. 2*B*).

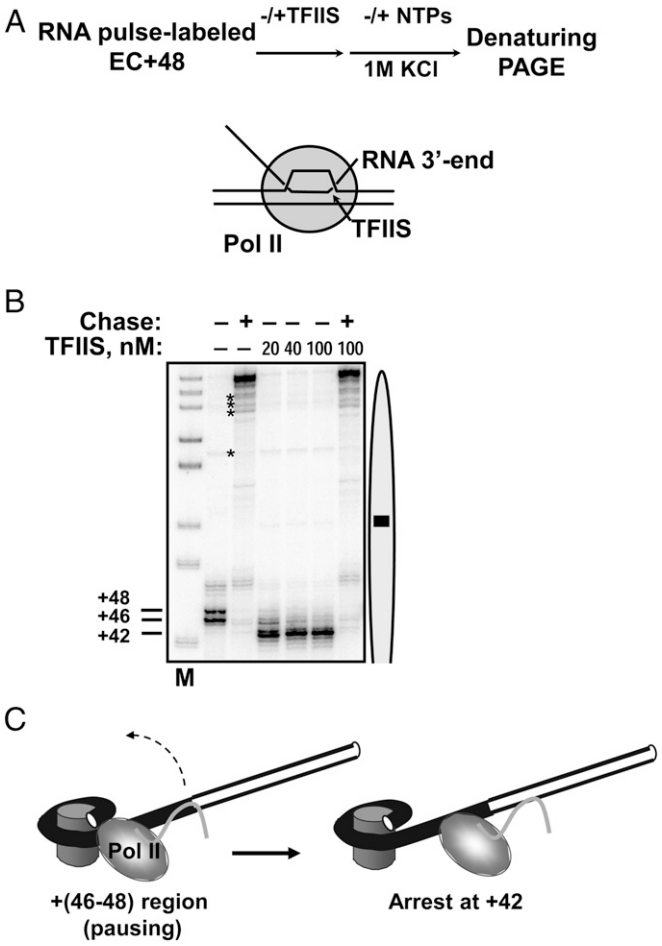

Fig. 2. Pol II EC arrested at positions +46 and +48 backtracks by 4 or 6 bp. (*A*) Experimental approach for mapping positions of the active center of Pol II on DNA. Pol II can backtrack, disengaging the 3′ end of RNA from the active center. The extent of backtracking was measured using TFIIS to stimulate RNA cleavage by Pol II at the active center. (*B*) Analysis of pulse-labeled RNA by denaturing PAGE. The chase was conducted in the presence of all NTPs at 1 M KCl to disrupt the nucleosome and allow unimpeded transcription. Note: TFIIS was present at concentrations that do not induce Pol II backtracking, as evidenced by the lack of its effect on the length of multiple arrested transcripts (indicated by asterisks). (*C*) Pol II backtracking (shown by dashed arrow) could result in formation of a DNA gap between Pol II and the nucleosome.

To determine the positions of the active center of Pol II, the +46 and +48 complexes were incubated in the presence of transcription elongation factor IIS (TFIIS). TFIIS is a transcription factor that strongly facilitates RNA cleavage at the active center of Pol II after backtracking (31). Incubation of the elongation complexes with TFIIS resulted in formation of homogeneous 42-mer RNA (Fig. 2*B*), indicating that both complexes were backtracked by 4 or 6 bp to the position +42. The nucleosomal +42, +46, and +48 complexes remain fully functional and can be reactivated upon nucleosomal removal in the presence of 1 M KCl (Fig. 2*B*). In summary, when Pol II encounters a strong nucleosomal barrier, it stops and backtracks by 4–6 bp. The backtracking could result in formation of a DNA gap between Pol II complex and the nucleosome (Fig. 2*C*), unless the nucleosomal DNA recoils back on the octamer surface.

The rotational orientation of Pol II at the +42 position after backtracking is incompatible with formation of the Ø loop (16). Therefore, we expected that nucleosomal DNA would be uncoiled from the octamer upstream of the +42 complex (Fig. 2*C*).

Accessibility of nucleosomal DNA in the +42 complex was analyzed using a restriction enzyme sensitivity assay (Fig. 3*A*). The nucleosome strongly protects DNA from digestion by restriction enzymes (32). In the elongation complex (EC) +42, only the AflIII site localized upstream of the active center (but not RsaI or MfeI sites localized downstream) is sensitive to cleavage (Fig. 3*B*). Thus, DNA in the +42 complex is uncoiled from the octamer upstream, but is tightly associated with histones downstream of the active center of the enzyme.

Close Encounter of Arrested RNAP with the Nucleosome Induces DNA Tension. The structures of various elongation complexes invading the nucleosome were further analyzed by single-hit DNase I footprinting (16) (Fig. 4*A*). Such analysis requires high amounts of homogeneous complexes that can be obtained only with model *E. coli* RNA polymerase (RNAP) that uses the Pol II-specific mechanism of transcription through chromatin in vitro (14, 16, 33). Currently Pol II cannot be used for these experiments because even in the most advanced experimental systems in vitro the efficiency of escape from assembled or promoter-initiated complexes to stable elongation complexes is quite low (it occurs on less than 20% of templates) (27, 34), and purification of the productive elongation complexes is extremely difficult. In contrast, RNAP forms a nearly homogeneous +48 complex during transcription through the 601 nucleosome (Fig. S3). After formation of the complex, RNAP immediately backtracks, forming a stable and functional +42 complex (Fig. S4). Therefore, as expected, RNAP recapitulates all critical properties of Pol II transcription through the high nucleosomal barrier.

The −39, −5, and +42 complexes have distinct mobilities in the native gel, confirming that all complexes are nearly homogeneous and have unique conformations. As expected (16), each elongation complex protects the ∼30-bp region and the nucleosome protects the ∼150-bp region from DNase I digestion (Fig. 4 *B* and *C*). The EC −39 and EC −5 complexes have structures that are very similar to the structures of similar complexes formed on the permissive 603 template (16). The footprint of each complex is a sum of the footprint's characteristic for the complex RNAP–DNA and nucleosome (Fig. 4 *B* and *C*).

RNAP completely uncoils upstream nucleosomal DNA in the +42 complex, whereas downstream DNA–histone interactions persist (Fig. 4 *B* and *C*). RNAP forms a tight complex with the nucleosome, with no DNase I-sensitive region between them. Two DNaseI-hypersensitive sites (hs-sites) are detected at the positions +96 and +102, surrounding the R3 DNA region that triggers arrest of Pol II at the +48 position (Fig. 1). The tight

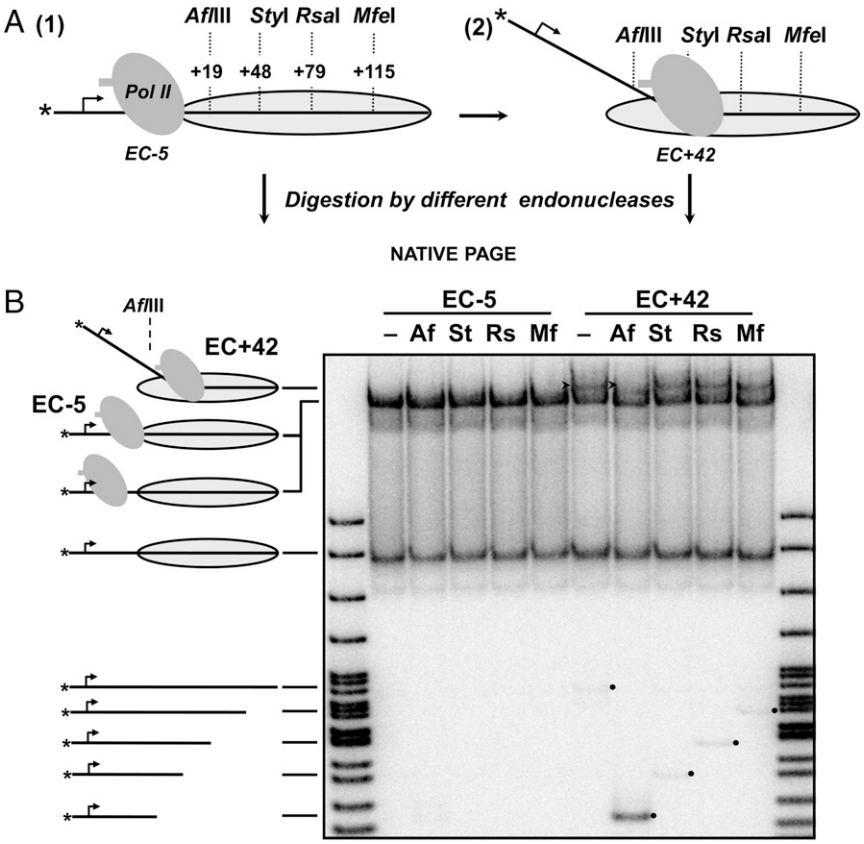

Fig. 3. DNA in the arrested +42 complex is partially uncoiled from the octamer upstream of Pol II. (*A*) Expected structures of the EC −5 and EC +42 (*1* and *2*) and accessibility of their DNA to various restriction endonucleases. Asterisks indicate the labeled DNA end. (*B*) Analysis of DNA sensitivity in the EC −5 and EC +42 to restriction endonucleases by native PAGE. Mobilities of the ECs, nucleosomes, and DNA in the gel are indicated. Mobility of EC +42 is indicated by arrowheads. Note that only EC +42 is sensitive to AflIII. All restriction enzymes are fully active, as indicated by complete digestion of histone-free DNA present in the samples (indicated by dots).

structure of the complex and the presence of the hs-sites suggest that after arrest, nucleosomal DNA is partially recoiled back on the histone octamer surface after backtracking of RNAP (Fig. 4*B*). RNAP collides with the promoter–distal end of the nucleosomal DNA, resulting in accumulation of DNA tension and formation of the hs-sites. The observation that the distorted region colocalizes with the PBS-R3 region is consistent with the key role of this sequence in formation of the high barrier to Pol II transcription (Fig. 1).

The structure of the arrested +42 complex is very similar to the structure of stalled EC +41 formed on the permissive 603 template (16). The striking similarities between the complexes formed at similar positions on the permissive 603 and nonpermissive 601 templates suggest that their structures are determined primarily by the position of the enzymes within the nucleosome. At the same time, EC formed on the permissive 603 nucleosomal template at similar positions (+49) has strikingly different properties: it is fully active, maintains its position on nucleosomal DNA, and partial DNA uncoiling from the octamer occurs downstream of the enzyme (16). The data suggest that RNAPs on the nonpermissive 601 nucleosome at position +48 are unable to form a stable Ø-loop intermediate, and instead backtrack by 4–6 bp to displace the upstream DNA from the octamer and to form the arrested EC +42. Thus, formation of the Ø loop and uncoiling of downstream DNA during Pol II transcription could occur during the single base pair step (+48 to +49).

Taken together, the data suggest that after arrest at +(46–48) positions in the nucleosome, the RNAPs backtrack to position +42. The enzymes remain functional, indicating that DNA–histone interactions themselves form the nucleosomal barrier to transcription. Backtracking of RNAPs is likely followed by recoiling of nucleosomal DNA on the surface of the histone octamer. Backtracking results in formation of a compact arrested +42 complex, with a close encounter between the RNAP and nucleosome. Formation of EC +42 is accompanied by formation of hypersensitive sites flanking the PBS-R3 sequence, most likely due to steric interference between the RNAP and promoter–distal end of nucleosomal DNA.

Structure of Pol II–Nucleosome Complex: Maintenance of Histone–Histone Interactions After Partial DNA Uncoiling from the Octamer. Next, the structure of the +42 complex of RNAP with nucleosome was determined using electron microscopy and single particle analysis (Fig. 5). The +42 EC has a combined molecular mass of about 545 kDa, making it difficult to observe them embedded in ice. Therefore, image contrast was enhanced using uranyl acetate negative staining (Fig. 5*A*). A total of 8,500 +42 EC particles were analyzed (Fig. 5 *B* and *C*). The preliminary 3D structure of the complex (Fig. 5*D*) was further refined. The final structure (Fig. 6) contains a larger (about 20 nm in diameter), and a smaller (about 14 nm in diameter) density. Fine structural features of the complex cannot be resolved at the obtained 22-Å resolution. Nevertheless, the obtained 3D structure allowed building of the model of the EC +42 elongation complex by docking of the crystal structures of RNAP (PDB code 4JKR) into the larger density, and nucleosome (PDB code 1KX5) into the smaller density (Fig. 6). Our EM data support the view

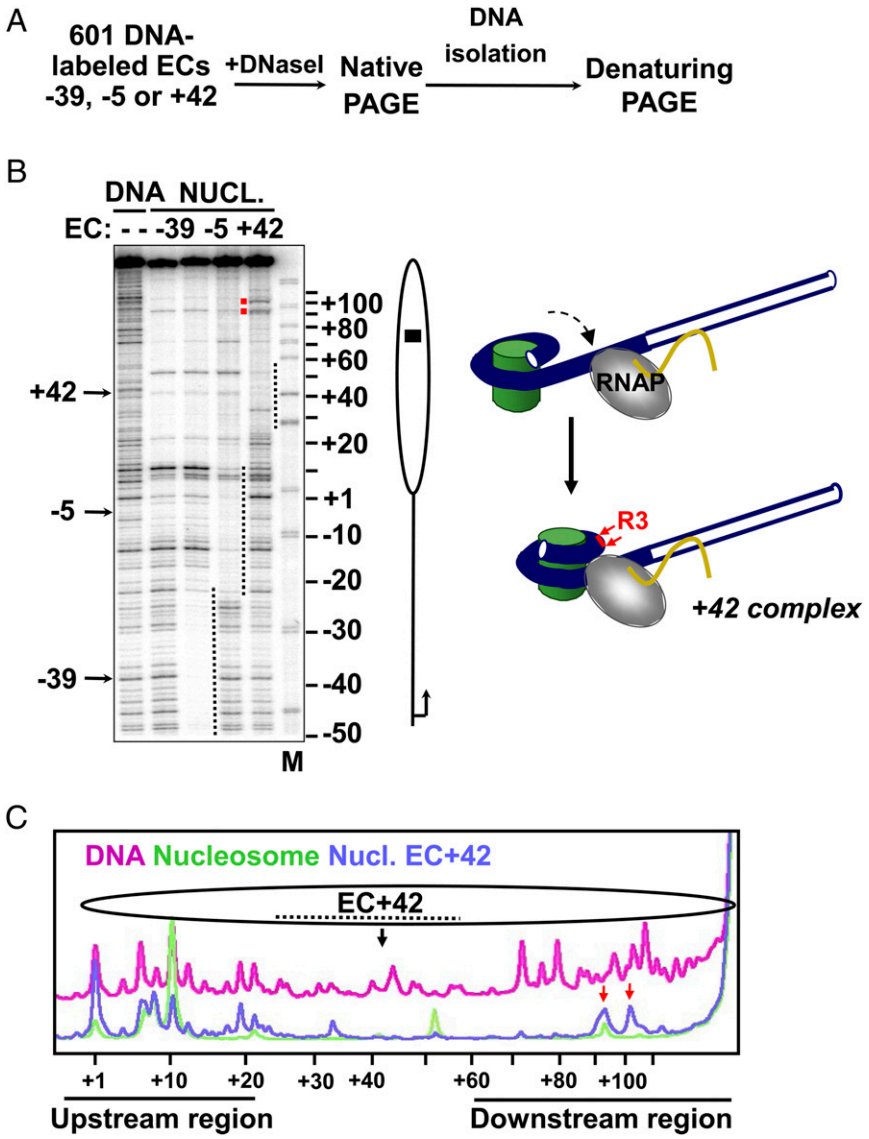

Fig. 4. Close encounter of arrested RNAP with the nucleosome induces formation of DNase I-hypersensitive DNA sites. Analysis of ECs formed on the 601 nucleosome by DNase I footprinting. (*A*) The experimental approach. ECs −39, −5, and +42 formed on the DNA end-labeled template were DNase I treated, separated by native PAGE, and the DNA was purified and analyzed by denaturing PAGE. (*B*, *Left*) Analysis of the end-labeled DNA by denaturing PAGE. Position of the nucleosome on the template, shown by an oval nucleosomal dyad is indicated. Footprints of the ECs are shown by dotted lines. DNA upstream of EC +42 is highly sensitive to DNase I, suggesting that it is nearly fully uncoiled from the octamer. Positions of two hypersensitive sites (+96/+102) around the R3 region are indicated. (*Right*) Tight structure of the +42 complex and the presence of DNase I-hypersensitive DNA sites suggest that nucleosomal DNA likely recoils on the octamer after backtracking of RNAP (shown by dashed arrow). (*C*) Quantitative analysis of the footprints shown in *B*.

that the EC +42 contains a single mononucleosome and one RNAP complex.

In the +42 complex, RNAP and the nucleosome are in close proximity to each other (Fig. 6). The spacer DNA connecting them is largely hidden by the proteins; thus the structure is consistent with DNase I footprinting data detecting no accessibility of the spacer DNA (Fig. 4). The tight structure of the complex is consistent with the proposal that in the arrested complex backtracking of RNAPs is followed by recoiling of nucleosomal DNA on the surface of histone octamer (Fig. 4*B*). Docking of a yeast Pol II elongation complex structure into the obtained model suggest that a similar complex can be formed by a eukaryotic Pol II (Fig. S5).

The most striking and surprising feature of the +42 complex is the opening of the DNA-interacting surface of the promoter–proximal histone dimer H2A/H2B. Indeed, the model of the +42 complex (Fig. 6 and Fig. S5) suggests that proximal H2A/H2B dimer is not stabilized by interactions with DNA or RNAP, but remains associated with the octamer. Furthermore, our previous data have shown that progression from the +42 to +49 complex is accompanied by full recoiling of nucleosomal DNA back on the surface of the dimer (16), suggesting that the dimer does not leave DNA before Pol II progresses more than 49 bp into the nucleosome. The stability of the dimer during transcription is remarkable, considering that the DNA-free octamer completely loses both H2A/H2B dimers in less than 1 s (35). Thus, the presence of nucleosomal DNA that remains partially coiled around the H3/H4 tetramer and promoter–distal H2A/H2B dimer results in a decrease of the rate of dissociation of the promoter–proximal dimer. The data suggest that binding of the promoter–proximal H2A/H2B dimer to H3/H4 tetramer in the +42 complex could be allosterically stabilized by the remaining

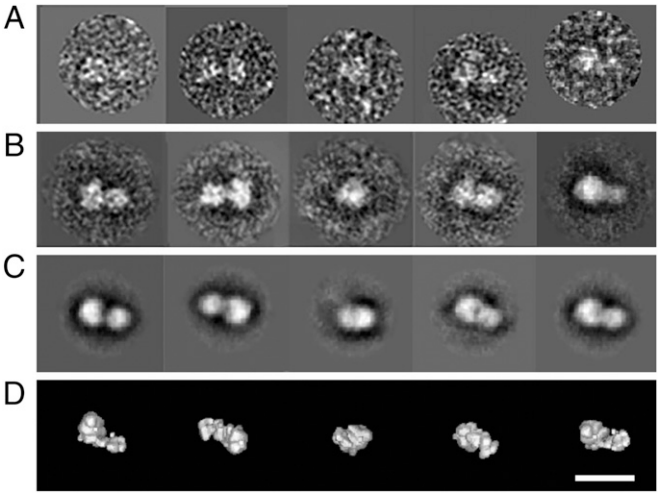

Fig. 5. Image processing of negatively stained EC +42. (*A*) Representative images corresponding to their respective class averages (*B*). (*B*) Class averages obtained by reference-free classification of particles. (C) Reprojections of 3D structure. (*D*) A 3D reconstruction of the +42 complex from negative-stain data. Views are produced with IMAGIC5. (Scale bar, 25 nm.)

DNA–histone interactions in the nucleosome. Because displacement of the dimer constitutes the first step to eviction of the entire histone octamer (36), this mechanism is likely important for nucleosome survival during various processes involving nucleosome remodeling.

The Mechanism of Formation and Overcoming the Nucleosomal Barrier to Transcription. Taken together with our previous footprinting studies of transcription-permissive nucleosomes, our data allow us to propose a detailed mechanism of Pol II transcription through the region of nucleosomal DNA [the +(40–50) region] that largely dictates the height of the nucleosomal barrier and nucleosome fate during transcription (14, 16) (Fig. 7 and Fig. S6).

As Pol II approaches a strong nucleosomal barrier [largely dictated by the R1, +(75–79) and by the R3, +(99–102) sequences, Fig. 1*B* and refs. 17, 28], it undergoes pausing or sequence-dependent arrest accompanied by Pol II backtracking along DNA (complex 2′, Figs. 2*C* and 7). The paused Pol II state (complex 2, Fig. 7) can be resolved by recoiling of DNA behind the enzyme back onto the surface of the histone octamer, forming a small loop on the nucleosome surface (complex 3, Ø loop) (16). In the complexes 2, 2′, and 3 Pol II induces partial tension in promoter–distal nucleosomal DNA (Figs. 4 and 7). However, only after formation of the complex 3 Pol II can drive partial unwrapping of promoter–distal end of nucleosomal DNA, clearing the way for further progression of the enzyme along DNA (complexes 4 and 5) (16). Unwrapping of the promoter–distal end of nucleosomal DNA and further Pol II progression can be blocked by certain DNA sequences; when present, they form strong DNA–histone interactions and block uncoiling of nucleosomal DNA from histones in front of the enzyme (complex 4, Figs. 1 and 7).

Discussion

Our data identify the transition from the +48 to +49 position as the key step during transcription through a nucleosome where Pol II makes a choice between arrest and further transcription. In the minimal system containing only Pol II and a nucleosome, this choice is dictated primarily by the sequence of nucleosomal DNA that determines the affinity of DNA–histone interactions and the probability of Pol II backtracking (Fig. S6). In particular, R3 DNA sequence at the +(99–102) region is critical for escape from the +48 position (Fig. 1 and Fig. S6).

The arrest at position +48 becomes nearly irreversible on the 601 nucleosome due to Pol II backtracking along DNA and partial recoiling of nucleosomal DNA on the octamer after backtracking (Fig. S6). The ability of Pol II to backtrack most likely depends on the DNA sequence immediately upstream of the active center of the enzyme and is typically reversible on DNA (37). However, recoiling of nucleosomal DNA on the octamer "locks" Pol II and makes backtracking irreversible (Fig. S6); a similar mechanism has been proposed previously (15).

The choice between the arrest and further transcription through the nucleosome can be affected by transcription factors and histone chaperones. Thus, elongation factor TFIIS that facilitates transcription through chromatin in vitro (15, 22) can facilitate escape from the arrested state (15, 26) (Fig. S6). Histone chaperone FACT facilitates transcription through chromatin via transient interaction with the open surface of histone octamer (20, 38). Thus, depending on the sequence of nucleosomal DNA and presence of dedicated proteins, various steps during transcription through a nucleosome can be rate limiting and possibly regulated in vivo.

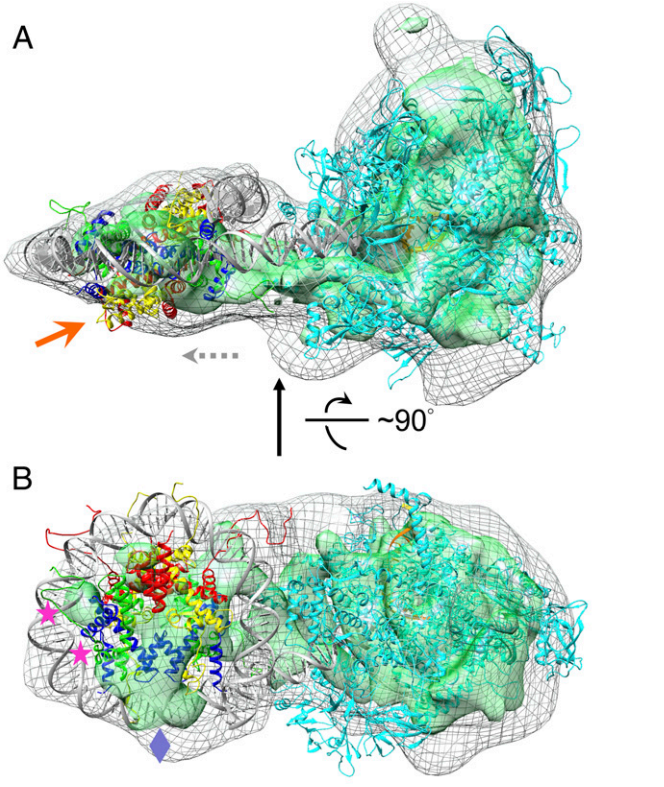

Fig. 6. Structure of the elongation complex arrested in position +42 in nucleosome. (*A*) Reconstitution of the EC +42 by fitting of nucleosome core particle and *E. coli* RNAP EC structures (PDB 1KX5 and 4JKR, respectively) into the electron densities of the complex, determined after negative staining. The isosurface of the 3D reconstruction is shown with a higher or lower threshold in gray mesh or in green, respectively (Fig. 5). Nucleosomal DNA was connected to DNA localized downstream of the active center of RNAP. The RNAP and RNA are depicted in cyan and orange, respectively. Histones H3, H4, H2A, and H2B are colored in blue, green, yellow, and red, respectively. The gray dotted and orange arrows indicate direction of transcription and promoter–proximal H2A/H2B dimer exposed into solution, respectively. (*B*) The structure was rotated by ~90° around the horizontal axis. The positions of DNaseI-hypersensitive sites on DNA are shown by asterisks. The nucleosomal dyad is indicated by purple diamond.

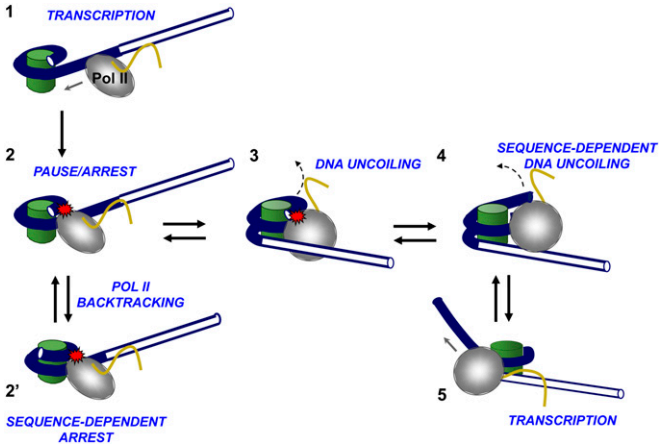

Fig. 7. The mechanism of transcription through the critical +(45–50) region of a nucleosome. As Pol II enters a nucleosome and approaches a strong nucleosomal barrier (step *1*), it is typically paused (*2*) or arrested (*2′*), depending on the sequence of nucleosomal DNA. Pol II can recover from arrest only with help of TFIIS that facilitates Pol II-induced RNA cleavage. Next, the DNA recoils behind the enzyme (*3*). In the complexes *2*, *2′*, and *3*, bulk of Pol II overlaps with nucleosomal DNA (red asterisk), likely inducing tension in nucleosomal DNA that could drive partial unwrapping of promoter–distal end of nucleosomal DNA (*4*), inducing transition into the productive complex (*5*). DNA uncoiling can be strongly inhibited by sequence-dependent DNA–histone interactions. Further transcription typically results in nucleosome recovery on DNA. Fig. S6 shows detail.

After overcoming the nucleosomal barrier, further Pol II transcription is typically accompanied by nucleosome survival mediated by formation of a small intranucleosomal DNA loop on the surface of the histone octamer (Ø loop, Fig. S6). The high efficiency of nucleosome survival has been puzzling because transcription by various RNA polymerases is accompanied by uncoiling of an extended DNA region (up to 80 bp) from the octamer (16, 39, 40), which is expected to induce immediate loss of an H2A/H2B dimer (35). The observed stability of the +42 complex containing a H2A/H2B dimer that is exposed into the solution (Fig. 6) suggests that binding of the H2A/H2B dimer to the H3/H4 tetramer could be allosterically stabilized (*Results*) and provides an explanation for the remarkable nucleosome stability of nucleosomal structure during various processes including transcription (16), replication (41), and ATP-dependent chromatin remodeling (42). Although one dimer is constitutively displaced from nucleosomes during transcription in vitro (27), this displacement likely occurs after transcription through the position +49 because the EC +49 contains both H2A/H2B dimers (43).

The +42/48 pausing described here is related to nucleosomal pausing observed in *Drosophila* (7) and yeast (43). In yeast, the primary nucleosomal barrier during transcript elongation by Pol II is encountered when the active center of the enzyme is +(40–55) bp in the nucleosome (43). A similar barrier is encountered by Pol II in *Drosophila* during transcription through nucleosomes localized more than ∼400 bp from the transcription start site (7). However, there are additional nucleosomal barriers at the positions −7 and +20 bp in *Drosophila*, characteristic for nucleosomes localized immediately downstream of the transcription start site (7).

Recent studies suggest that the density of Pol II complexes along the transcribed genes likely dictates the critical outcomes of transcription through chromatin—the height of nucleosomal barrier (21, 26, 44) and the extents of histone displacement and exchange (6, 21, 45, 46). At the same time, multiple factors including histone modifications, histone variants, histone chaperones, and chromatin remodelers further modify the histone dynamics on transcribed genes (refs. 1–3, 47 for review). Some of these factors interact with tumor suppressors (48) and present important targets for the development of anticancer drugs (49).

Materials and Methods

DNA Templates. The plasmids containing 601 and 603 sequences were described previously (14). The 601 nucleosomal template for Pol II was prepared as described (14), where the 147-bp nucleosome positioning sequence was amplified by PCR and digested with TspRI (NEB) for further ligation to the assembled Pol II EC −39. To prepare the templates for *E. coli* RNAP transcription, the nucleosome positioning sequences digested by TspRI (NEB) was ligated through the TspRI site to the T7A1 promoter-bearing fragment (33). The ligated product was reamplified with 5′ end-labeled primers, gel purified, and assembled into nucleosomes. Details regarding the design of the templates and primer sequences will be provided upon request.

Protein Purifications and Nucleosome Assembly. Hexahistidine-tagged *E. coli* RNAP was purified according to published protocols (50). GreB protein was purified as described (51). TFIIS was purified as described (52). Nucleosomes were reconstituted on end-labeled 226-bp DNA templates by histone octamer transfer from the chicken -H1 erythrocyte donor chromatin DNA at a 1:3 DNA-to-chromatin ratio (16). -H1 chromatin also provides unlabeled DNA that serves as a competitor for nucleosome formation. This approach allows semiquantitative comparison of relative free energies (affinities) of histone–DNA interactions (16, 53). The nucleosomes were analyzed in a native gel (16); the mobility of a nucleosome in the gel reflects nucleosome positioning.

Transcription. *E. coli* RNAP elongation complexes containing 11-mer RNA (EC −39) were formed on preassembled nucleosomal templates as described (33). In the case of experiments with labeled RNA, EC −39 was pulse labeled in the presence of [α-^{32}P]-GTP (3,000 Ci/mmol, PerkinElmer Life Sciences). Then EC −39 was extended in the presence of a subset of NTPs to form EC −5 (Fig. S1). In the case of the footprinting experiments, all steps were performed in solution. In the case of experiments involving labeled RNA and GreB treatment, EC −5 was immobilized on Ni-NTA-agarose (33). After extensive washes, the complexes were eluted from Ni-NTA beads in the presence of 100 mM imidazole and transcription was continued in solution. To form EC +48 the EC −5 was extended in the presence of 10 μM NTPs at 25 °C for 15 min in TB300 (20 mM Tris·HCl pH 8.0, 5 mM $MgCl_2$, 2 mM β-ME, 300 mM KCl). Then the immobilized ECs were washed in TB40 (20 mM Tris·HCl pH 8.0, 5 mM $MgCl_2$, 2 mM β-ME, 40 mM KCl), eluted by 100 mM imidazole, and incubated with GreB. Labeled RNA was purified and separated by denaturing PAGE.

Pol II assembled elongation complex containing 9-mer RNA (EC −41), formed as described (14), was immobilized on Ni-NTA beads and extended in the presence of 20 μM ATP and GTP to form EC −39, washed, and eluted by 100 mM imidazole. EC −39 was ligated to the nucleosomal template through the TspRI site and transcribed to EC −5 and EC +48 as described for *E. coli* RNAP.

Because the complex of RNAP, stalled in position +42 of the 603 nucleosome, is more structurally homogeneous than the spontaneously arrested +42 complex on 601 nucleosome, the stalled +42 603 complex was used for the structural analysis. To obtain EC +42 stalled complex, the EC −5 was formed as described previously (16) and the sample was dialyzed against 2× TB300 in a cold room for 2 h to remove ATP in solution. The EC −5 was then extended in the presence of 20 μM CTP, UTP, and GTPs and 1 mM 3′ ATP (TriLink BioTechnologies) at 25 °C for 4 min to form EC +42.

DNaseI Footprinting. DNaseI footprinting was carried out at a final concentration of 2.5 μg/mL of labeled templates in the presence of 10-fold weight excess of unlabeled -H1 chicken erythrocyte chromatin in TB100 (20 mM Tris·HCl pH 8.0, 5 mM $MgCl_2$, 2 mM β-ME, 100 mM KCl). DNaseI was added to the final concentration 20–50 units/mL for 30 s in 37 °C after formation of the desired ECs. The reactions were terminated by adding EDTA to 10 mM. The samples were resolved in a native gel (54). Gel fragments containing desired complexes were cut, DNA purified, and analyzed by denaturing PAGE. The gels were quantified using a PhosphorImager.

Electron Microscopy. To reveal the EC +42 3D structure, negative staining of samples with 1% uranyl acetate was used. Freshly prepared EC +42 was applied to the carbon-coated glow-discharged grid, stained for 30 s with uranyl acetate, and air dried. Grids were studied in JEOL 2100 TEM, operated at 200 kV at low-dose conditions. Micrographs were captured by the Gatan CCD camera. The initial 3D reconstitution was obtained from random conical tilt (RCT) data with −45/0 degrees tilt. Using EMAN2 software 2,500 tilted

pairs were picked up, using the e2RCTboxer.py command. The correction for contrast transfer function of the microscope was performed in EMAN2 using command e2ctf.py. Reference free class averages (Fig. 5*A*) were obtained using the e2refine2d.py command. The 3D structure of EC +42 (Fig. 5*D*) was revealed with the resolution of 30 Å. An additional 6,000 particles were added to the set and three structurally different sets of images were separated using IMAGIC5. One set was RNA polymerase alone (5% of particles). Two other sets differed by the position of the nucleosome: more distant from RNA polymerase (85% of all particles) and the ones where the nucleosome is closer to the RNAP (10% of all particles). The most representative model was further refined using 85% of particles to obtain a final 3D structure of EC +42 at a resolution of 22 Å, estimated by Fourier shell correlation method at 0.5 (Fig. 6). Multimeric statistical analysis (MSA) of aligned particles produced eigen images (Fig. S7) and demonstrated that there are two distinct parts of the complex. The contour level was chosen based on an average protein density of 810 Da/nm^3 and volume corresponded to ~545 kDa for EC +42. The docking of the molecular model of EC +42 complex (see below) into obtained 3D density resulted in cross-correlation coefficient 0.73.

Modeling the RNAP–Nucleosome Complex EC +42. To model the +42 RNAP–nucleosome complex, the X-ray structure of *Thermus thermophilus* RNAP elongation complex (55) was at first combined with the X-ray structure of a nucleosome core particle (56) by elongating its downstream DNA duplex with a segment of straight B-DNA and connecting it to various corresponding positions along the nucleosomal DNA while respecting the correct DNA geometry and chemical bonding. The *T. thermophilus* RNAP was then replaced by the *E. coli* RNAP structure (57) via structure superposition; the structures of the two enzymes are very similar (Fig. S8). The modeling pipeline was based on University of California San Francisco Chimera (58) and Nucleic Acid Builder (NAB) (59) programs. The obtained family of models was fitted automatically into an experimentally obtained electron density map using the Chimera EM fitting utility (the atomistic model was converted into a simulated electron density map with 30-Å resolution for fitting purposes and extensive search with 40 different trial starting placements was done). The best model was selected based on maximum cross-correlation of electron densities. In the obtained model, the active center of the RNAP is in position +42; the downstream duplex of DNA enters the nucleosome at position +71 (3 bp before the position of the dyad axis). Finally, the structure of yeast Pol II elongation complex (PDB ID 1Y1W) (60) was superimposed on the *E. coli* RNAP structure to obtain the Pol II +42 elongation complex (Fig. S5).

ACKNOWLEDGMENTS. We thank John Widom for plasmids containing the nucleosome positioning sequences; David Clark, Mark Gartenberg, and Don Luse for suggestions and critical reading of the manuscript; and the Supercomputing Center of Lomonosov Moscow State University for using the computational facilities (61). Studies using radioactively labeled materials were supported in part by NIH Grant GM58650 (to V.M.S.). Single-particle microscopy studies were supported by the Russian Science Foundation (RSF 14-24-00031).

1. Smolle M, Workman JL, Venkatesh S (2013) reSETting chromatin during transcription elongation. *Epigenetics* 8(1):10–15.
2. Das C, Tyler JK (2013) Histone exchange and histone modifications during transcription and aging. *Biochim Biophys Acta* 1819(3-4):332–342.
3. Zentner GE, Henikoff S (2013) Regulation of nucleosome dynamics by histone modifications. *Nat Struct Mol Biol* 20(3):259–266.
4. Kristjuhan A, Svejstrup JQ (2004) Evidence for distinct mechanisms facilitating transcript elongation through chromatin *in vivo*. *EMBO J* 23(21):4243–4252.
5. Schwabish MA, Struhl K (2004) Evidence for eviction and rapid deposition of histones upon transcriptional elongation by RNA polymerase II. *Mol Cell Biol* 24(23):10111–10117.
6. Lee CK, Shibata Y, Rao B, Strahl BD, Lieb JD (2004) Evidence for nucleosome depletion at active regulatory regions genome-wide. *Nat Genet* 36(8):900–905.
7. Weber CM, Ramachandran S, Henikoff S (2014) Nucleosomes are context-specific, H2A.Z-modulated barriers to RNA polymerase. *Mol Cell* 53(5):819–830.
8. Guenther MG, Levine SS, Boyer LA, Jaenisch R, Young RA (2007) A chromatin landmark and transcription initiation at most promoters in human cells. *Cell* 130(1):77–88.
9. Muse GW, et al. (2007) RNA polymerase is poised for activation across the genome. *Nat Genet* 39(12):1507–1511.
10. Zeitlinger J, et al. (2007) RNA polymerase stalling at developmental control genes in the *Drosophila melanogaster* embryo. *Nat Genet* 39(12):1512–1516.
11. Mavrich TN, et al. (2008) Nucleosome organization in the *Drosophila* genome. *Nature* 453(7193):358–362.
12. Brown SA, Imbalzano AN, Kingston RE (1996) Activator-dependent regulation of transcriptional pausing on nucleosomal templates. *Genes Dev* 10(12):1479–1490.
13. Izban MG, Luse DS (1991) Transcription on nucleosomal templates by RNA polymerase II in vitro: Inhibition of elongation with enhancement of sequence-specific pausing. *Genes Dev* 5(4):683–696.
14. Bondarenko VA, et al. (2006) Nucleosomes can form a polar barrier to transcript elongation by RNA polymerase II. *Mol Cell* 24(3):469–479.
15. Kireeva ML, et al. (2005) Nature of the nucleosomal barrier to RNA polymerase II. *Mol Cell* 18(1):97–108.
16. Kulaeva OI, et al. (2009) Mechanism of chromatin remodeling and recovery during passage of RNA polymerase II. *Nat Struct Mol Biol* 16(12):1272–1278.
17. Hall MA, et al. (2009) High-resolution dynamic mapping of histone-DNA interactions in a nucleosome. *Nat Struct Mol Biol* 16(2):124–129.
18. Brown SA, Kingston RE (1997) Disruption of downstream chromatin directed by a transcriptional activator. *Genes Dev* 11(23):3116–3121.
19. Izban MG, Luse DS (1992) Factor-stimulated RNA polymerase II transcribes at physiological elongation rates on naked DNA but very poorly on chromatin templates. *J Biol Chem* 267(19):13647–13655.
20. Hsieh FK, et al. (2013) Histone chaperone FACT action during transcription through chromatin by RNA polymerase II. *Proc Natl Acad Sci USA* 110(19):7654–7659.
21. Kulaeva OI, Hsieh FK, Studitsky VM (2010) RNA polymerase complexes cooperate to relieve the nucleosomal barrier and evict histones. *Proc Natl Acad Sci USA* 107(25): 11325–11330.
22. Kim J, Guermah M, Roeder RG (2010) The human PAF1 complex acts in chromatin transcription elongation both independently and cooperatively with SII/TFIIS. *Cell* 140(4):491–503.
23. Guermah M, Palhan VB, Tackett AJ, Chait BT, Roeder RG (2006) Synergistic functions of SII and p300 in productive activator-dependent transcription of chromatin templates. *Cell* 125(2):275–286.
24. Carey M, Li B, Workman JL (2006) RSC exploits histone acetylation to abrogate the nucleosomal block to RNA polymerase II elongation. *Mol Cell* 24(3):481–487.
25. Bintu L, et al. (2012) Nucleosomal elements that control the topography of the barrier to transcription. *Cell* 151(4):738–749.
26. Jin J, et al. (2010) Synergistic action of RNA polymerases in overcoming the nucleosomal barrier. *Nat Struct Mol Biol* 17(6):745–752.
27. Kireeva ML, et al. (2002) Nucleosome remodeling induced by RNA polymerase II: Loss of the H2A/H2B dimer during transcription. *Mol Cell* 9(3):541–552.
28. Hsieh FK, Fisher M, Ujvári A, Studitsky VM, Luse DS (2010) Histone Sin mutations promote nucleosome traversal and histone displacement by RNA polymerase II. *EMBO Rep* 11(9):705–710.
29. Gaykalova DA, et al. (2011) A polar barrier to transcription can be circumvented by remodeler-induced nucleosome translocation. *Nucleic Acids Res* 39(9):3520–3528.
30. Kulaeva OI, Hsieh FK, Chang HW, Luse DS, Studitsky VM (2013) Mechanism of transcription through a nucleosome by RNA polymerase II. *Biochim Biophys Acta* 1829(1):76–83.
31. Fish RN, Kane CM (2002) Promoting elongation with transcript cleavage stimulatory factors. *Biochim Biophys Acta* 1577(2):287–307.
32. Polach KJ, Widom J (1999) Restriction enzymes as probes of nucleosome stability and dynamics. *Methods Enzymol* 304:278–298.
33. Walter W, Kireeva ML, Studitsky VM, Kashlev M (2003) Bacterial polymerase and yeast polymerase II use similar mechanisms for transcription through nucleosomes. *J Biol Chem* 278(38):36148–36156.
34. Murakami K, et al. (2013) Architecture of an RNA polymerase II transcription preinitiation complex. *Science* 342(6159):1238724.
35. Feng HP, Scherl DS, Widom J (1993) Lifetime of the histone octamer studied by continuous-flow quasielastic light scattering: Test of a model for nucleosome transcription. *Biochemistry* 32(30):7824–7831.
36. Bintu L, et al. (2011) The elongation rate of RNA polymerase determines the fate of transcribed nucleosomes. *Nat Struct Mol Biol* 18(12):1394–1399.
37. Komissarova N, Kashlev M (1997) Transcriptional arrest: *Escherichia coli* RNA polymerase translocates backward, leaving the 3′ end of the RNA intact and extruded. *Proc Natl Acad Sci USA* 94(5):1755–1760.
38. Belotserkovskaya R, et al. (2003) FACT facilitates transcription-dependent nucleosome alteration. *Science* 301(5636):1090–1093.
39. Chang HW, et al. (2013) Structural analysis of the key intermediate formed during transcription through a nucleosome. *Trends Cell Mol Biol* 8:13–23.
40. Bednar J, Studitsky VM, Grigoryev SA, Felsenfeld G, Woodcock CL (1999) The nature of the nucleosomal barrier to transcription: Direct observation of paused intermediates by electron cryomicroscopy. *Mol Cell* 4(3):377–386.
41. Randall SK, Kelly TJ (1992) The fate of parental nucleosomes during SV40 DNA replication. *J Biol Chem* 267(20):14259–14265.
42. Mueller-Planitz F, Klinker H, Becker PB (2013) Nucleosome sliding mechanisms: New twists in a looped history. *Nat Struct Mol Biol* 20(9):1026–1032.
43. Churchman LS, Weissman JS (2011) Nascent transcript sequencing visualizes transcription at nucleotide resolution. *Nature* 469(7330):368–373.
44. Chang HW, et al. (2014) Analysis of the mechanism of nucleosome survival during transcription. *Nucleic Acids Res* 42(3):1619–1627.
45. Dion MF, et al. (2007) Dynamics of replication-independent histone turnover in budding yeast. *Science* 315(5817):1405–1408.
46. Rufiange A, Jacques PE, Bhat W, Robert F, Nourani A (2007) Genome-wide replication-independent histone H3 exchange occurs predominantly at promoters and implicates H3 K56 acetylation and Asf1. *Mol Cell* 27(3):393–405.
47. Weber CM, Henikoff S (2014) Histone variants: Dynamic punctuation in transcription. *Genes Dev* 28(7):672–682.
48. Wen H, et al. (2014) ZMYND11 links histone H3.3K36me3 to transcription elongation and tumour suppression. *Nature* 508(7495):263–268.
49. Garcia H, et al. (2013) Facilitates chromatin transcription complex is an "accelerator" of tumor transformation and potential marker and target of aggressive cancers. *Cell Reports* 4(1):159–173.

50. Artsimovitch I, Svetlov V, Murakami KS, Landick R (2003) Co-overexpression of *Escherichia coli* RNA polymerase subunits allows isolation and analysis of mutant enzymes lacking lineage-specific sequence insertions. *J Biol Chem* 278(14): 12344–12355.
51. Vassylyeva MN, et al. (2007) The carboxy-terminal coiled-coil of the RNA polymerase beta′-subunit is the main binding site for Gre factors. *EMBO Rep* 8(11):1038–1043.
52. Ujvári A, Hsieh FK, Luse SW, Studitsky VM, Luse DS (2008) Histone N-terminal tails interfere with nucleosome traversal by RNA polymerase II. *J Biol Chem* 283(47): 32236–32243.
53. Thåström A, Lowary PT, Widom J (2004) Measurement of histone-DNA interaction free energy in nucleosomes. *Methods* 33(1):33–44.
54. Walter W, Kireeva ML, Tchernajenko V, Kashlev M, Studitsky VM (2003) Assay of the fate of the nucleosome during transcription by RNA polymerase II. *Methods Enzymol* 371:564–577.
55. Vassylyev DG, Vassylyeva MN, Perederina A, Tahirov TH, Artsimovitch I (2007) Structural basis for transcription elongation by bacterial RNA polymerase. *Nature* 448(7150):157–162.
56. Davey CA, Sargent DF, Luger K, Maeder AW, Richmond TJ (2002) Solvent mediated interactions in the structure of the nucleosome core particle at 1.9 a resolution. *J Mol Biol* 319(5):1097–1113.
57. Zuo Y, Wang Y, Steitz TA (2013) The mechanism of E. coli RNA polymerase regulation by ppGpp is suggested by the structure of their complex. *Mol Cell* 50(3):430–436.
58. Pettersen EF, et al. (2004) UCSF Chimera: A visualization system for exploratory research and analysis. *J Comput Chem* 25(13):1605–1612.
59. Bomble YJ, Case DA (2008) Multiscale modeling of nucleic acids: Insights into DNA flexibility. *Biopolymers* 89(9):722–731.
60. Kettenberger H, Armache KJ, Cramer P (2004) Complete RNA polymerase II elongation complex structure and its interactions with NTP and TFIIS. *Mol Cell* 16(6): 955–965.
61. Sadovnichy V, Tikhonravov A, Voevodin V, Opanasenko V (2013) Lomonosov: Supercomputing at Moscow State University in *Contemporary High Performance Computing: From Petascale Toward Exascale*, ed Vetter JS (Chapman & Hall/CRC Computational Science, Boca Raton, FL), pp 283–307.